Journal of Trends in Computer Science and Smart Technology (ISSN: 2582-4104)
www.irojournals.com/tcsst/

Design of an Aperture-Coupled Patch Antenna for Unmanned Aerial Vehicle Communication

Nikkila Paul P.[1], Anita Jones Mary Pushpa T.[2]

[1]Research Scholar, [2]Assistant Professor, Karunya Institute of Technology and Sciences (KITS), Coimbatore, India.

Email: [1]nikkilapaul@karunya.edu.in, [2]anitajones@karunya.edu

Abstract

The aperture-coupled patch antenna, characterized by its low profile and cost-effectiveness, has been developed for Unmanned Aerial Vehicle (UAV) communication in this research. A significant advantage of the aperture-coupled patch antenna is its simplified design process compared to other antenna types. This configuration minimizes complexity of transmission lines while enhancing the radiation pattern and plane. In the context of UAV communication, the aperture-coupled patch antenna is crucial, faciliating efficient communication between users. It effectively transmits electromagnetic energy and minimizes interference, thereby improving communication efficiency in UAV applications. The performance of the designed aperture-coupled patch antenna has been evaluated through simulation results, demonstrating high gain, an optimal radiation pattern, a low Voltage Standing Wave Ratio (VSWR), and a strong polarization ratio.

Keywords: Aperture-Coupled Patch Antenna, Patch Antenna; Unmanned Aerial Vehicles Communication; High Efficiency; Antenna Gain.

1. Introduction

In Unmanned Aerial Vehicle (UAV) communication, the antenna plays an important role. It helps to transmit and receive signals between the UAV and the ground station. The major aspect of the antenna in UAV communication is the communication range. The antenna determines the range of communication between the ground station and the UAV. Effective

DOI: https://doi.org/10.36548/jtcsst.2025.2.001
Received: 02.04.2025, received in revised form: 30.04.2025, accepted: 14.05.2025, published: 23.05.2025

communication occurs within a specific communication range. The communication range varies based on the following factors.

- Antenna type
- Antenna Localization
- Frequency Selection
- Power Selection
- Environmental Conditions

Various types of antennas are involved in UAV communication systems, such as monopole, dipole, patch, helical and yagiuda antennas. The characteristics of each antenna include radiation pattern, gain, size and frequency range, which will be selected based on the requirements of the UAV application.

For efficient UAV communication, the antenna must be placed correctly. This helps to reduce interference and increase the signal strength. The selection of frequency is another important factor for efficient communication. Different frequency bands are available, such as 2.4GHz, 5.8GHz and licensed bands. When selecting the frequency band, it should be ensured that it is compatible for efficient communication. In general, the antenna affects signal quality and data rate in UAV communication. High-gain antennas help to increase the quality of received signal strength by placing the antenna in the appropriate position on the UAV. The link budget of the antenna determines the gain or loss in the communication system. It includes antenna gain, transmission power, receiver sensitivity, cable losses, and path loss. A good link budget provides highly efficient signal strength for effective communication. Miniaturized and lightweight antennas are often preferred for UAV applications. Printed and flexible antennas are more suitable for integrating compact antennas into UAVs and provide efficient performance.

Figure 1 shows that the UAV to ground communication model contains a UAV and a base station. There is wireless communication between the UAV and the base station. The UAV contains sensor nodes, antenna, and an operating system. Based on the antenna type, the communication efficiency will vary.

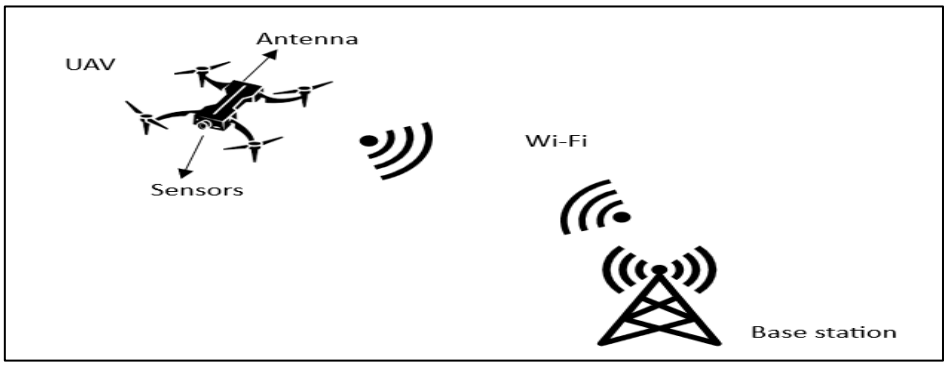

Figure 1. UAV to Ground Communication Model

Overall, antennas are vital components in UAV communication systems, enabling reliable and efficient data transmission between the UAV and the ground station or other communication devices, with the proper selection of the antenna based on size, weight, frequency range, placement, and link budget.

The aperture-coupled patch antenna is the most important type of microstrip patch antenna design. This aperture coupled patch antenna improves impedance matching, reduces radiation from feedlines, and increases isolation between the feed and the radiating element. While designing the aperture-coupled patch antenna, the design of the patch must be considered. The main focus of this approach is to determine the resonant frequency, thickness, and permittivity based on the operating frequency range. For the determination of the resonant frequency, the antenna shape must be identified based on the requirements. The selection of substrate material with a low loss tangent helps to obtain signal propagation. The aperture helps to connect the patch and feedline of the antenna. The coupling efficiency can be improved based on the selection of the size and shape of the antenna. The microstrip line helps to connect the aperture and feedline. The impedance matching and radiation characteristics must be identified based on the feedline's length and width. The ground plane shields the RF and acts as a reflector for the radiating element. The designed antenna is implemented in simulation software, which helps to identify the performance of the antenna based on parameters such as impedance matching, radiation pattern, gain, and bandwidth. Changing the design parameters helps to improve the antenna's performance. Once the performance of the newly designed antenna is analyzed and found to be satisfactory, the fabrication and testing process will be conducted. In the simulation part, the comparison of various antennas is performed which helps to analysis of the performance of the aperture-coupled patch antenna.

Aperture-coupled patch antennas are widely used in various applications, including wireless communications, radar systems, and satellite communications. Their design can be customized to meet specific frequency, bandwidth, and gain requirements, making them suitable for different operating environments.

2. Related works

Meng et al., [1] proposed UAV integrated sensing and communication for wireless 6G networks. The proposed scheme enhanced the coverage range of the mobile node and provided an efficient communication. The scheme concentrated the sensing and communication with the help of unmanned aerial vehicles. Do et al., [2] analysed the various techniques involved in mmWave UAV aided communication networks. Additionally, intelligent learning-based approaches were employed to overcome the research issues in mmWave communication networks. Miao et al., [3] introduced intelligent reflecting surfaces in unmanned aerial vehicles to reduce security issues in the network. The method reduced fading with the help of IRS assisted UAV and enhanced security.

Ouamri et al., [4] explained the importance of UA multiple antennas assisted small cell networks. The approach used the matern clustered process between the small base station and unmanned aerial vehicles. The carrier frequency of 28 GHz was used, and the power ranges from 30dbm available for the small base station and 24dBm for the UAV scheme were obtained. Ge et al., [5] suggested the enhanced intelligent reflecting surface to reduce path loss and interference. During data transmission between the ground and unmanned aerial vehicles, there is a possibility of high interference due to the line-of-sight paths. Hence, the beamforming and intelligent reflecting surface of UAV were integrated to enhance communication between the end users. Wang et al., [6] introduced the super formula ultra-wideband antenna with a size of 30mm X 40mm. This reduced interference in WLAN communications. The results produced an impedance bandwidth of 2.7 GHz to 14.1 GHz. It achieving high gain and accuracy.

Dong et al., [7] proposed a secure hybrid beamforming framework to improve signal quality, secure communication and reduce interference between the ground station and unmanned aerial vehicles. Amodu et al., [8] integrated the terahertz communication with unmanned aerial vehicles for 6G enabled communication networks. The most difficult factor was maintaining the line-of-sight path between the UAV nodes with high mobility. The review provided the challenges and issues faced while integrating UAVs with terahertz

communication. Lu et al., [9] analyzed the UAV-assisted mmWave model that incorporates high beamforming. This reduced UAV jitter and improved performance with efficient communication. Yao et al., [10] discussed the UAV flight trajectory, which helped to solve the UAV optimization problem. Additionally, a reconfigured intelligent surface was introduced for efficient communication between the ground and UAV, improving energy efficiency in the wireless network by 145%.

Yin et al., [11] introduced a mixed integer nonlinear program with a consensus-based bundle algorithm for long distance communication. The approach helped transmit t data from the UAV to the ground station and achieved higher efficiency. Zhang et al., [12] proposed atuning beamwidth directional antenna for the UAV system, which increased the radiation pattern and radiation gain. Wang et al., [13] investigated the multi-user intelligent reflecting surface with backscatter for efficient communication. The proposed scheme jointly optimized the UAV, base station, and IRS for highly reliable communication between ground users and UAV user. Licea et al., [14] proposed the fixed wing unmanned aerial vehicles achieved high efficiency. Byun et al., [15] explained the importance of unmanned aerial vehicles integrated with reconfigurable intelligent surfaces for maintaining successful line of sight paths. Additionally, the scheme improved the spectral efficiency by varying the phase shifts.

Zheng et al., [16] proposed a novel shared-aperture dual-band array with a tightly coupled buffering layer (TCBL) achieves low profile, broad bandwidth, and strong cross-band isolation in 0.69–0.96 GHz and 1.47–2.7 GHz bands. Ma et al., [17] proposes a dual-band shared-aperture antenna combining a 2.4 GHz microwave patch and a 60 GHz millimeter-wave transmitarray (TA) using structure reuse. A mushroom-type metasurface enhances bandwidth (15.4% at 5.40–6.30 GHz and 12.9% at 4.13–4.70 GHz), suppresses mutual coupling, and provides over 22 dB isolation. The design achieves over 5 dB RCS reduction, with experimental results aligning well with simulations, making it suitable for radar and stealth applications. He et al., [18] introduce a novel dual-band shared-aperture array with a tightly coupled buffering layer (TCBL) enabling a low-profile design and broad bandwidths of 32.7% (0.69–0.96 GHz) and 59.0% (1.47–2.7 GHz). The TCBL serves dual roles: reactance compensation in the low band and bandwidth enhancement in the high band, while naturally suppressing cross-band interference. TR et al., [19] designed an EBG antenna for ISM band applications at 2.4 GHz and 5.8 GHz. It integrates an EBG ring structure on an FR-4 substrate to enhance radiation performance and minimize interference. With dimensions of 70 × 80 mm²

and optimized feed-line and material parameters, it achieves a return loss below –10 dB and a VSWR between 1 and 2 for effective impedance matching. Cheng et al., [20] present a dual-band co-aperture antenna covering 2.09–11.61 GHz (138.9%) and 21.6–29.6 GHz (31%) with a compact size of $0.76 \times 0.76 \times 0.37\ \lambda_0$.

3. Methodology

Designing an aperture-coupled patch antenna for UAV communication involves several critical steps. The specification determination encompasses factors such as frequency range, bandwidth, gain, polarization, and substrate material. Figure 2 illustrates the vertical over patch box.

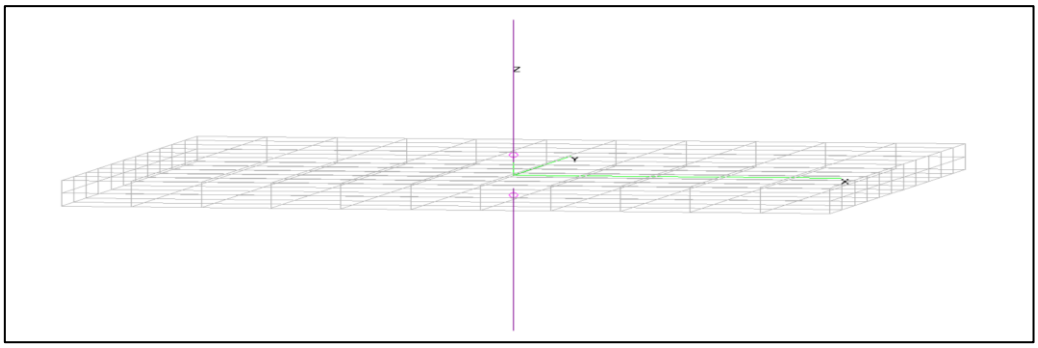

Figure 2. Vertical Geometry Patch Antenna

Figure 3 shows the rectangular patch antenna with a microstrip feed line. The aperture coupled patch antenna is shown in Figure 4. The rectangular patch and aperture are integrated into the patch antenna. The microstrip feed line is used for transferring the signal. The rectangular patch coupled with aperture provides efficient communication in UAV communications.

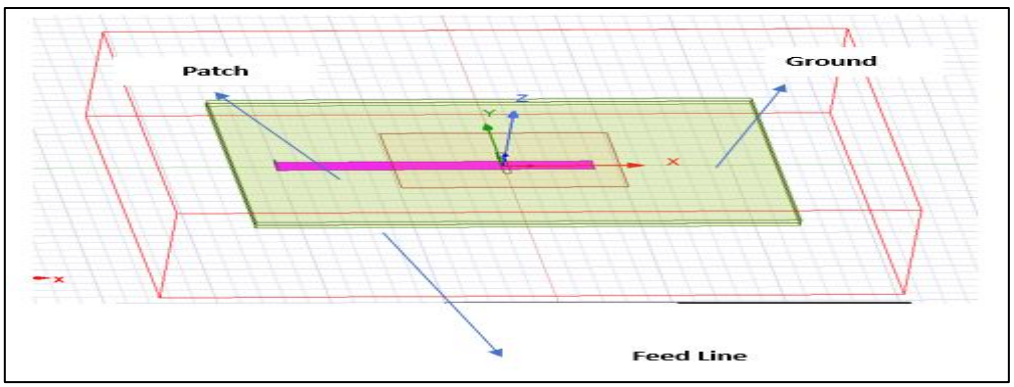

Figure 3. Rectangular Patch Antenna

- **Design of Rectangular Patch antenna**

The length, height, and width of the rectangular patch antenna are calculated using the resonant frequency and analysed using the fundamental mode (λ/2) operation.

$$L_{rp} \approx 0.49\lambda_0/\sqrt{\varepsilon_r} \quad (1)$$

Equation 1 is used to find the length of the rectangular patch (L_{rp}), where λ_0 denotes the free space wavelength and ε_r is the relative permittivity.

$$W_{rp} = \frac{c}{2f_0}\sqrt{\frac{2}{\varepsilon_r+1}} \quad (2)$$

Equation 2 denotes the width of the rectangular patch $(W_{rp}), where$ c is the speed of the signal and f_0 denotes the free space frequency.

$$h_{rp} \leq \frac{0.3V_0}{2\pi r\sqrt{\varepsilon_r}} \quad (3)$$

The length, width, and height of the patch antenna are designed by using the equations 1, 2 and 3.

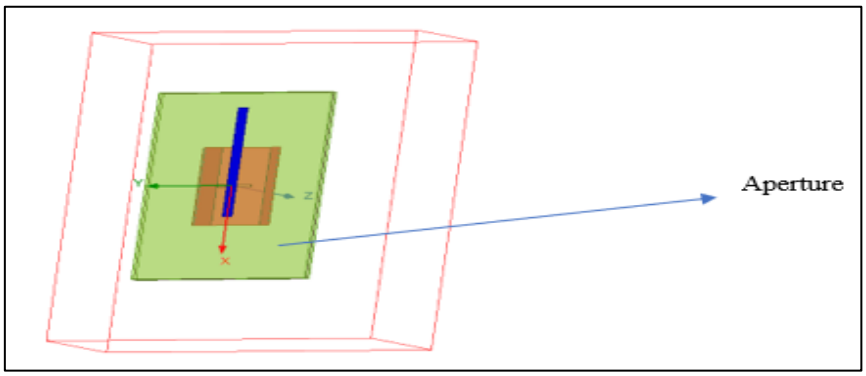

Figure 4. Rectangular Patch Aperture Coupled

- **Design of Aperture Coupling**

The next step is the designing of aperture coupling with the rectangular patch antenna.

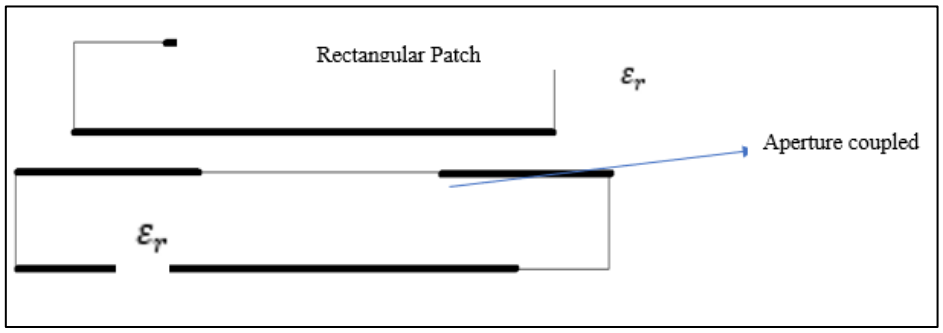

Figure 5. Aperture Coupled Patch Antenna

Figure 5 shows the aperture-coupled patch antenna. The frequency of the aperture coupling varies from 2.45 GHz to 2.55 GHz. The bandwidth varies from 0.068GHz to 0.075GHz.

- **Microstrip Feed line**

The microstrip feed line ($z_0 = 55\Omega$) is placed perpendicular to the center of the microstrip slot. The feed line width is 5.2mm and the length is 2.3mm. The electric length of the microstrip is 10.7 degrees.

- **Substrate Selection**

The substrate parameter, dielectric constant is designed here.

$$D_e = \frac{\varepsilon}{\varepsilon_0} \tag{4}$$

The stub length is designed after the feed line is designed. This helps to reduce the unwanted reactance of aperture.

- **Algorithm**

Step -1: Calculate Patch Dimensions:

Use Equation 1 to calculate the length of the rectangular patch (Lrp) and use Equation 2 to calculate the width of the rectangular patch (Wrp):

Step -2: Design Patch Height

Use Equation 3 to calculate the maximum allowable height of the patch (hrp) based on your specific requirements.

Step -3: Aperture Coupling Design:

Step -4: Microstrip Feed Line Design:

Set the desired impedance of the microstrip feed line (z0). Calculate the electric length of the microstrip based on the desired phase shift.

Step -5: Substrate Selection:

Calculate the substrate dielectric constant (De) using Equation 4 based on the desired relative permittivity (εr) and the vacuum permittivity (ε0).

Step -6: Stub Length Design:

Design the stub length (Lstub) after the feed line is designed to reduce unwanted reactance of the aperture.

Step -7: Finalization:

Verify the design to obtain the gain, impedance, VSR and reflection coefficient values.

4. Results and Discussion

The proposed antenna is designed using ANSYS software. The first step is to select the HFSS model and then the patch antenna is designed with the feed line inserted later to the aperture in the rectangular patch. This helps to improve the gain, return loss, directivity, Voltage Standing Wave Ratio (VSWR) and impedance. This antenna will be more suitable for unmanned aerial vehicle communication. In unmanned aerial vehicle, the communication will be more faster and more secure compared to other modes of transmission media.

The input parameters are shown in table 1.

Table 1. Simulation Parameters

Parameter	Dimensions (mm)	Aperture Feed
Substrate height	1.6	Lower: FR4
	1.6	Upper: Roger

Height	1.6	-
Patch length (L)	38	32.9
Patch width (W)	46	41.9
Ground length (6H+L)	85	-
Ground width (6H+W)	80	-
Feed length (fL)	23.5	47.5
Feed width (fW)	1	8

The effective relative permittivity is defined in equation 5.

$$\varepsilon_{reff} = \frac{\varepsilon_r+1}{2} + \frac{\varepsilon_r-1}{2}(1 + 12\frac{h}{w})^2 \quad (5)$$

The effective length extension is calculated by using equation 6.

$$\Delta L = \frac{0.412h(\varepsilon_{reff}+0.3)(\frac{w}{h}+0.264)}{(\varepsilon_{reff}-0.264)(\frac{w}{h}+0.68)} \quad (6)$$

The effective length is calculated by using equation 7.

$$L_{eff} = \frac{c}{2f_0\sqrt{\varepsilon_{reff}}} \quad (7)$$

The effective length can be rewritten as follows:

$$L_{eff} = L + 2\Delta L \quad (8)$$

The ground length of the patch is defined in equation 9.

$$L_g = 6h + L \quad (9)$$

The width of the patch is defined in equation 10.

$$W_g = 6h + W \quad (10)$$

Antenna gain is defined as the sum of directivity and efficiency. Return loss is defined as the ratio of feeding power from the starting point with respect to the amount of return or reflection to the starting point. Directivity is defined as the concentration of power which that is radiated in the field. Antenna impedance can be measured at the edges or terminals of the antenna. It is defined as the ratio of voltage to current at the terminals of an antenna. VSWR is defined as the maximum voltage to the minimum voltage.

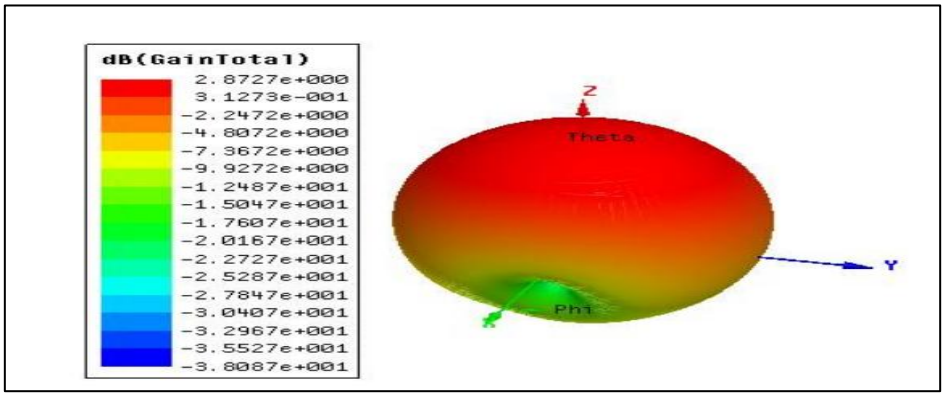

Figure 6. Gain Plot

Figure 6 shows the gain obtained using the simulation software. High antenna gain is achieved due to the aperture coupled patch antenna. In the aperture coupling, the feed width is significantly wider at 8 mm. A wider feed improves the bandwidth and potentially the gain of the antenna by enhancing the coupling between the feed and the radiating patch. The obtained peak gain is 6.49 dB.

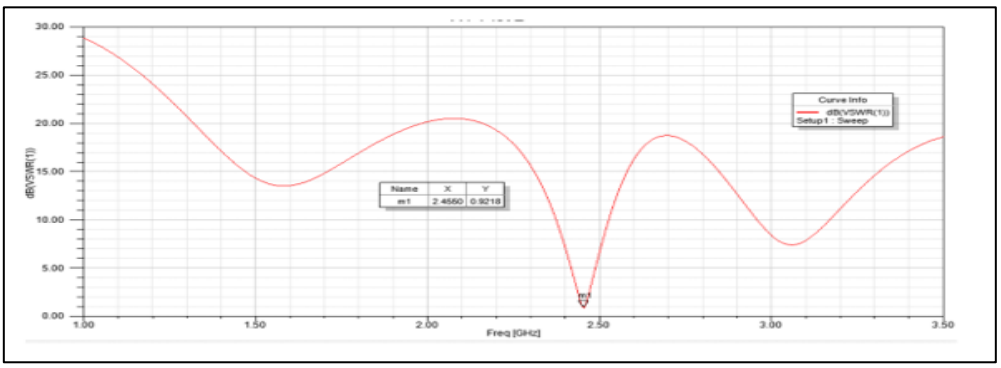

Figure 7. VSWR

Figure 7 represents the VWSR (Voltage Wave Standing Ratio). VSWR measures the antenna's impedance-matching to the transmission line. Ideally, VSWR should be close to 1:1. A lower VSWR means better impedance matching, reducing signal reflection. In this case, the

aperture-coupled patch antenna has a VSWR of 1.38 dB indicating more efficient power transfer.

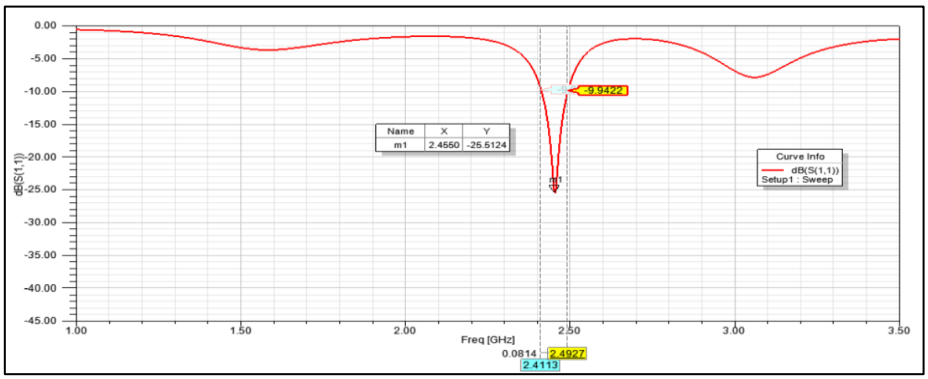

Figure 8. Return loss

Figure 8 indicates the results of return loss. Return loss helps to measure power transferred and reflected from the antenna instead of being radiated. A more negative value indicates better impedance matching and less reflection. The lowest point on the curve occurs at approximately 2.4550 GHz, with a reflection coefficient of -25.5124 dB. This point represents the resonant frequency, where the antenna is most efficiently radiating energy with minimal reflection. The return loss at the resonant frequency is -33.34 dB, which indicates a very good impedance match. Generally, a return loss lower than -10 dB is considered good, so -33.34 dB is excellent.

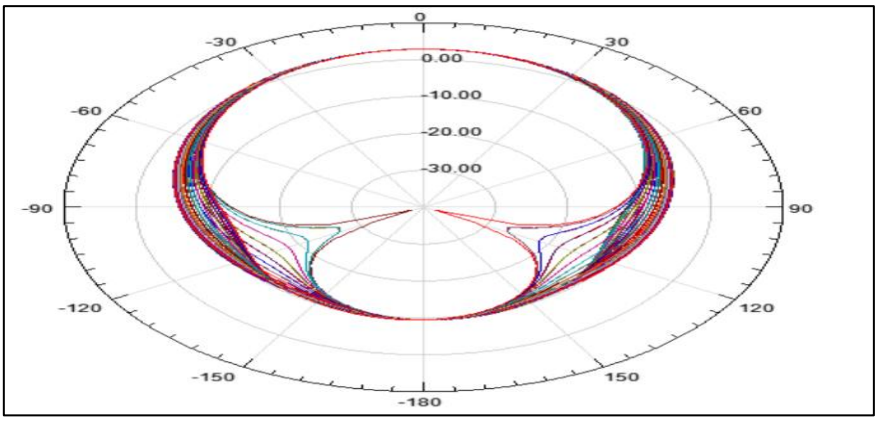

Figure 9. Radiation Pattern

Figure 9 shows the radiation pattern for the proposed antenna. The lower gain with the coupled feed suggests it may have a more omnidirectional radiation pattern or different energy distribution. It achieves a 6.49 dB wider radiation pattern with higher gain. The aperture-

coupled patch antenna has a broader radiation pattern, which is more suitable for UAV applications, and it achieves wider coverage.

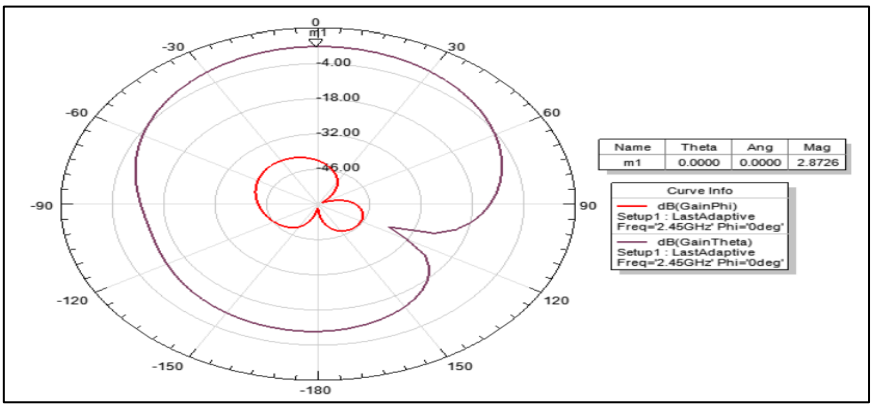

Figure 10. E Plane Pattern

Figure 10 represents the E-Plane radiation pattern. The E-Plane refers to the plane containing the electric field vector (E) and the direction of maximum radiation. The vertical plane shows how the electric field strength varies as a function of angle in that plane. In the E-plane pattern, the main lobe typically points in the direction perpendicular to the patch surface and represents the broader radiation. The main lobe is used to measure the radiation focus in one direction. A narrower main lobe indicates the antenna is more directional, radiating more power in one direction which provides high gain. The angular width of the main lobe is where the power is half of its maximum value (3 dB down).

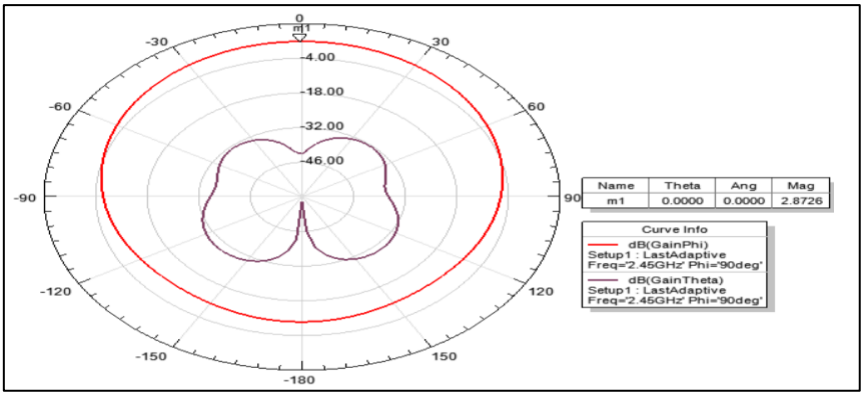

Figure 11. H-Plane Pattern

Figure 11 represents the H-Plane radiation pattern. The H-Plane refers to the plane containing the magnetic field vector (H) and the direction of maximum radiation. This is usually the horizontal plane, perpendicular to the E-plane. In the H-plane, the main lobe

represents the radiation of the antenna in the plane perpendicular to the electric field. If the antenna has good performance, this main lobe will be broad, indicating the ability to radiate over a wider horizontal area. The H-plane pattern shows a more focused and narrower beam horizontally. It provides the antennas with higher gain, where radiation is more concentrated in a specific direction. The beamwidth in the H-plane is an important factor for antennas used in UAV communication systems that require wide horizontal coverage. This antenna design minimizes cross-polarization for better signal clarity.

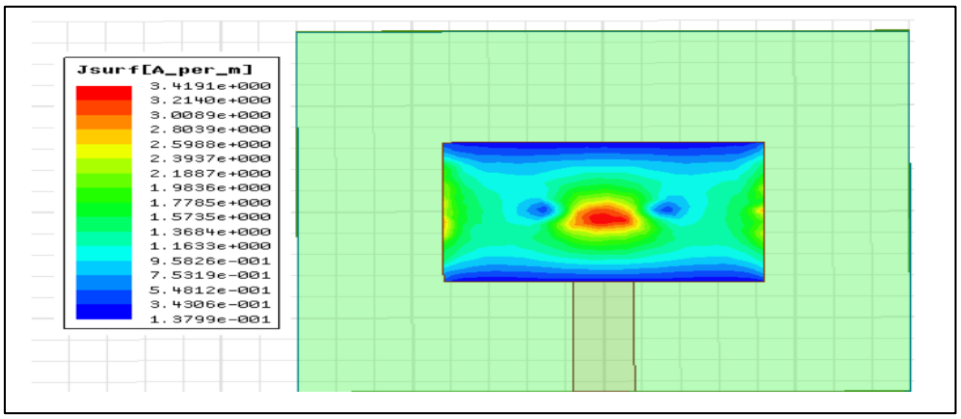

Figure 12. Current Distribution

Figure 12 shows the current distribution of the current magnitude and phase on the antenna surface at the resonant frequency. It provides a uniform current distribution across the patch. The current distribution helps to optimize performance by adjusting the patch dimensions, feed position, and material selection to improve efficiency, gain, and bandwidth. The current distribution is slightly altered due to the interaction between the feed structure and the patch surface. The feed energy couples into the patch via the feed mechanism, helping to create different current paths compared to a directly fed patch. The distribution pattern may show broader areas of current flow, which may impact the impedance matching, bandwidth, and gain of the antenna. The coupled feed tends to smooth the current distribution across a broader area, it is beneficial in improving bandwidth and making the antenna more broadband in nature.

Table 2. Result Analysis

Parameters	Aperture Coupled Patch Antenna
Resonant Frequency	2.45 GHZ

Return Loss	-33.34 dB
VSWR	1.38 dB
Bandwidth	0.046 GHZ
Peak Gain	6.49 dB

The result obtained for the aperture-coupled patch antenna is shown in table 2. The high gain, high efficiency and high radiated power, and high VSWR improve the performance of the communication between the unmanned aerial vehicles.

5. Conclusion

The aperture-coupled patch antenna offers an efficient communication solution for unmanned aerial vehicle (UAV) applications. The primary advantage of this antenna design is its low profile and compact size, facilitating easy integration into vehicle communication systems. This antenna is capable of providing directional radiation, enhancing communication effectiveness. Additionally, it demonstrates high efficiency in converting input energy into radiated energy, which contributes to reduced power consumption in UAV communications. The aperture-coupled patch antenna also exhibits a low interference profile. Overall, the combination of its low profile, high efficiency, directional radiation, and other beneficial characteristics makes the aperture-coupled patch antenna an excellent choice for UAV communication applications, ensuring reliable and efficient wireless connectivity for unmanned aerial vehicles.

References

[1] Meng, Kaitao, Qingqing Wu, Jie Xu, Wen Chen, Zhiyong Feng, Robert Schober, and A. Lee Swindlehurst. "UAV-enabled integrated sensing and communication: Opportunities and challenges." IEEE Wireless Communications (2023).

[2] Do, Quang Tuan, Demeke Shumeye Lakew, Anh Tien Tran, Duc Thien Hua, and Sungrae Cho. "A Review on Recent Approaches in mmWave UAV-aided Communication Networks and Open Issues." In 2023 International Conference on Information Networking (ICOIN), IEEE, 2023, 728-731.

[3] Miao, Jiansong, Tongjie Li, Shanling Bai, Shi Yan, and Yan Zhao. "Secrecy Capacity Enhancement in Active IRS-Assisted UAV Communication System." Sensors 23, no. 9 (2023): 4377.

[4] Ouamri, Mohamed Amine, Daljeet Singh, Mohamed Ali Muthanna, Ahcen Bounceur, and Xingwang Li. "Performance analysis of UAV multiple antenna-assisted small cell network with clustered users." Wireless Networks 29, no. 4 (2023): 1859-1872.

[5] Ge, Yimeng, Jiancun Fan, Geoffrey Ye Li, and Li-Chun Wang. "Intelligent reflecting surface-enhanced UAV communications: Advances, challenges, and prospects." IEEE Wireless Communications (2023).

[6] Wang, Huai-Zhen, and Yong-Gang Zhou. "A superformula-based UWB conformal antenna with two notched bands for UAV applications." In Second International Conference on Electronic Information Engineering and Computer Communication (EIECC 2022), vol. 12594, SPIE, 2023, 393-399.

[7] Dong, Runze, Buhong Wang, Kunrui Cao, and Jiwei Tian. "Hybrid Beamforming for Secure Transmission of Massive MIMO UAV Communication Networks." IEEE Systems Journal (2023).

[8] Amodu, Oluwatosin Ahmed, Chedia Jarray, Sherif Adeshina Busari, and Mohamed Othman. "THz-enabled UAV communications: Motivations, results, applications, challenges, and future considerations." Ad Hoc Networks 140 (2023): 103073.’

[9] Lu, Conghui, and Peng Chen. "Robust channel estimation scheme for multi-UAV mmWave MIMO communication with jittering." Electronics 12, no. 9 (2023): 2102.

[10] Yao, Yuanyuan, Ke Lv, Sai Huang, Xuehua Li, and Wei Xiang. "UAV trajectory and energy efficiency optimization in RIS-assisted multi-user air-to-ground communications networks." Drones 7, no. 4 (2023): 272.

[11] Yin, Dong, Xuan Yang, Huangchao Yu, Siyuan Chen, and Chang Wang. "An Air-to-Ground Relay Communication Planning Method for UAVs Swarm Applications." IEEE Transactions on Intelligent Vehicles (2023).

[12] Zhang, Hongtao, and Xueyuan Li. "Directional antennas modelling and coverage analysis for UAV networks with blockage effects in urban environment." Transactions on Emerging Telecommunications Technologies 34, no. 4 (2023): e4737.

[13] Wang, Jinming, Sai Xu, Shuai Han, and Liang Xiao. "UAV-Powered Multi-User Intelligent Reflecting Surface Backscatter Communication." IEEE Transactions on Vehicular Technology (2023).

[14] Licea, Daniel Bonilla, E. Moises Bonilla, Mounir Ghogho, and Martin Saska. "Energy-efficient fixed-wing UAV relay with considerations of airframe shadowing." IEEE Communications Letters (2023).

[15] Byun, Yongsuk, Hyunsoo Kim, Seungnyun Kim, and Byonghyo Shim. "Channel Estimation and Phase Shift Control for UAV-carried RIS Communication Systems." IEEE Transactions on Vehicular Technology (2023).

[16] Zheng, Qi, Jinyu Ma, Zhongdian Wu, and Peyman PourMohammadi. "Dual-broadband high-isolation circularly polarized Low-RCS shared-aperture antenna array based on mushroom-type metasurface." Optics Communications 574 (2025): 131127.

[17] Ma, Zi Long, Yi Tang, Quan Xue, Wenquan Che, and Kai Xu Wang. "Dual-Band Shared-Aperture Antenna Hybridizing Patch and Transmitarray with Large Frequency Ratio and Wideband Characteristics." IEEE Transactions on Antennas and Propagation (2025).

[18] He, Yi, Shaodong Wang, Gengming Wei, Can Ding, and Y. Jay Guo. "A New Buffering Scheme for Shared-Aperture Dual-Band Base Station Antenna Array Utilizing Tight-Coupling Concept." IEEE Transactions on Antennas and Propagation (2025).

[19] TR, Ganesh Babu. "Flexible EBG Structure Antenna for ISM Band Applications." IRO Journal on Sustainable Wireless Systems 7, no. 1 (2025): 57-72.

[20] Cheng, Jia, Tianyu Gao, Dongpeng Han, and Changfei Zhou. "Dual-Band Shared-Aperture Antenna with Pattern and Polarization Diversity." Applied Sciences 15, no. 2 (2025): 878.